RAPID COMMUNICATIONS

PHYSICAL REVIEW A VOLUME 35, NUMBER 9 MAY 1, 1987

Growth of fractal crystals in amorphous $GeSe_2$ films

Gy. Radnoczi and T. Vicsek
Institute for Technical Physics, P.O. Box 76, H-1325 Budapest, Hungary

L. M. Sander and D. Grier
Physics Department, The University of Michigan, Ann Arbor, Michigan 48109
(Received 22 September 1986)

We present the first study of fractal growth in a solid-solid phase transition. A highly ramified randomly branched crystalline phase was obtained by heating thin amorphous $GeSe_2$ films. Our result for the fractal dimension of the above structure, $D \sim 1.7$, is in agreement with that of two-dimensional diffusion-limited aggregates. Possible mechanisms resulting in fractal growth are discussed.

The unstable growth of interfaces typically results in rich geometrical patterns. One commonly studied pattern-forming system consists of a solidification front advancing into an undercooled melt of the pure substance. Solidification from an undercooled melt is a diffusion-limited process because motion of the interface is determined by a diffusion field, the temperature, which satisfies the Laplace equation in the quasistationary approximation (that is, in the limit of long diffusion length). If the interfacial surface tension has substantial crystalline anisotropy, the interface often forms ordered dendrites. Random fluctuations, however, can dominate the pattern-forming process, leading to disordered structures.[1-3]

Diffusion-limited aggregation (DLA) introduced by Witten and Sander[4] is a simple model which seems to possess some of the most important features of growth processes described by the Laplace equation. The random dendritic patterns generated in the DLA model can be regarded as approximations to the solution of the Laplace equation with moving boundaries. The relevance of DLA for the description of the formation of fractal objects[5] in nature has been demonstrated by a few experiments in hydrodynamics,[6-9] electrodeposition,[10-13] and sputtered deposition.[14]

When comparing experimental results with those of DLA, one has to take into account factors which make the analogy less straightforward. First of all, in such experimental situations as viscous fingering or solidification, the long-scale behavior is determined by continuum equations rather than by the dynamics of individual molecules (as in DLA). In addition, experimentally obtained patterns depend strongly on the surface tension which is not incorporated into the original version of diffusion-limited aggregation. Correspondingly, the anisotropy of the surface tension is not considered in DLA and it is probably the lack of the anisotropy which leads to the fractal growth.

This explains why few examples are known of fractal growth in crystallization (where the anisotropy usually dominates pattern formation). In this Rapid Communication we investigate the geometry of the crystalline phase of $GeSe_2$ advancing into amorphous $GeSe_2$ films. In this case, effects caused by the anisotropic surface tension are expected to be small because the new phase is polycrystalline with preferred growth directions randomly distributed.

Thin films of $GeSe_2$ were prepared by vacuum evaporation of polycrystalline $GeSe_2$ from a tantalum boat in a vacuum of 10^{-3} Pa. Thin carbon layers mounted on a hexagonal copper grid served as a substrate. During deposition the substrate was kept at room temperature. The thickness and the deposition rate were measured with a quartz microbalance to be 70 nm and 0.8 nm/min, respectively. From the electron diffraction patterns of the sample we concluded that the microstructure of the film was amorphous with a short correlation length.

After having obtained the amorphous layers we annealed them in air at successively increased temperatures from 140 °C to up to 220 °C in four steps each of 30 min. These temperatures are well below the $GeSe_2$ glass transition temperature of 265 °C.[15] We then took transmission electron micrographs of the sample using a JEM 100U electron microscope.

When the films were heat treated at 220 °C a crystalline phase started growing from the copper rods of the supporting mesh. The crystallization front moved from the rods toward the center of the mesh leaving a partially polycrystalline film behind. The polycrystalline microstructure of the new phase showed up in the 75-keV diffraction patterns taken from the sample which indicate a typical crystallite size of about 100 Å. In most of the cases the crystallization started in concentric rings (Figs. 1 and 2), which was probably due to the particular method by which the samples were prepared.

The crystalline phase resembles a forest with a typical tree size on the order of 10 μm [Figs. 3(a) and 4(a)]. These trees closely resemble shapes arising in two-dimensional DLA simulations.

To compare the observed structures with the DLA model, we measured the fractal dimension of the crystalline phase. Having digitized the electron micrographs in Figs. 3(a) and 4(a) with an Oculus image processor, we logarithmically subtracted the background and thresholded the resulting image to obtain a 256×256 pixel bit map. By counting the number $n(r)$ of dark pixels at a radius r from the center of mass and assuming the scaling law

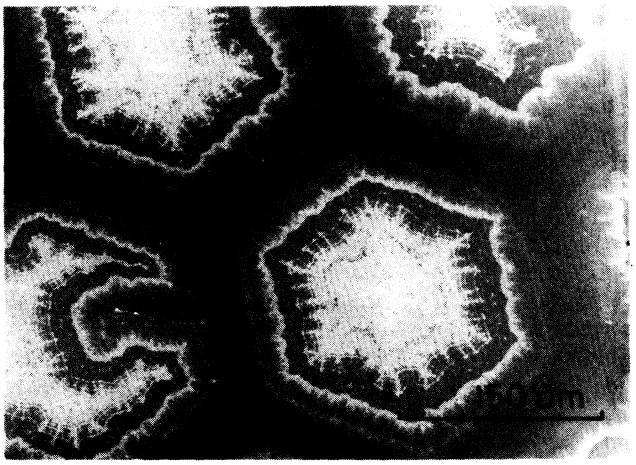

FIG. 1. Picture of the heat-treated (220 °C, 1 h) $GeSe_2$ film previously deposited on carbon layer supported by a honeycomb copper mesh. This image was obtained by a transmission electron microscope. The crystallization starts in concentric rings.

$n(r) \sim r^{D-1}$ for r less than the radius of gyration, we extract the fractal dimension D [see Figs. 3(b) and 4(b)]. This method was found to be accurate to 1% for a picture of a Sierpinski gasket for which the fractal dimension is known analytically.

For the two main branches in Fig. 3, we measured $D = 1.73 \pm 0.05$ while for the branch in Fig. 4, $D = 1.69 \pm 0.05$. The error bars are estimated by repeating the digitization in various orientations. The difference in the figures can be attributed to the different contrast levels in the photographs.

The origin of fractal structure in DLA is an example of the Mullins-Sekerka instability: The more advanced the tip of a branch is the more effectively it catches diffusing particles and the faster it grows. This is analogous to the motion of the solidification front in an undercooled melt: If the interface bulges into the liquid at some point it moves into a relatively cooler region and advances faster. A different but analogous mechanism applies to our experiment. In our case, crystallization starts at warmer places and slows down as the interface advances into cooler regions. The instability probably arises from the corresponding mechanism which occurs in the isothermal solidification of a liquid mixture,[16,17] where concentration gradients limit the growth.

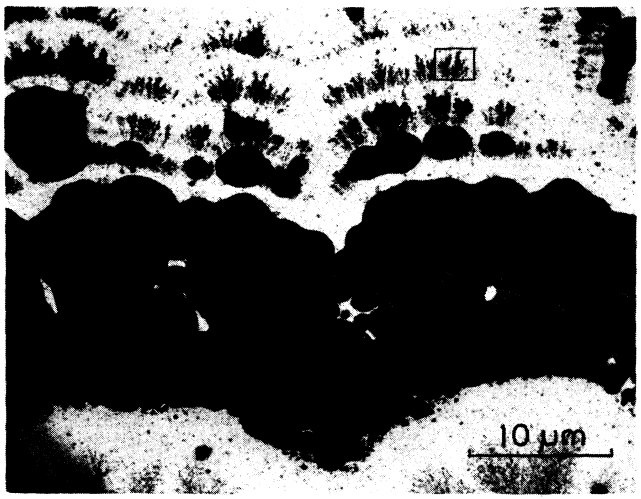

FIG. 2. Fragment of Fig. 1. Two types of crystallization fronts appear in the amorphous regions: (i) dendritic growth, (ii) spherolitic crystallization (the darkest part of the picture). Figs. 3 and 4 are enlargements from the interior of the small box.

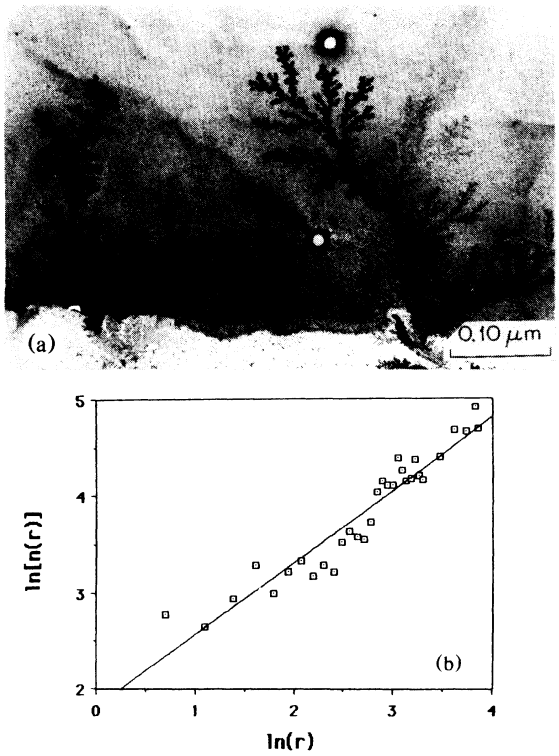

FIG. 3. (a) Part of the forest of dendritic crystals grown in the first zone. These trees are polycrystalline with a characteristic crystallite size less than 1000 Å. This size is considerably smaller than the width of the branches. (b) The two new branches have fractal dimension $D = 1.73 \pm 0.05$.

Let us assume that the main components of our system, Ge and Se, are not present with their stochiometric concentrations, e.g., $C_{Se} > C_{Ge}/2$. Then, if the temperature is higher than the amorphous-solid transition temperature, crystallization of $GeSe_2$ begins at the places which are somewhat warmer or contain more nucleation centers. The crystallizing phase expells excess Se so that the amorphous region near the interface becomes further enriched in Se. This excess of Se must diffuse away into the amorphous phase before further crystallization can occur. Concentration gradients are greatest at the most advanced parts of the interface, and so these regions grow fastest.

The observed branch thickness for the fractal trees is the range 20–50 Å, which is comparable to the crystallite size measured by electron diffraction. These branches are considerably thinner than the amorphous film from which

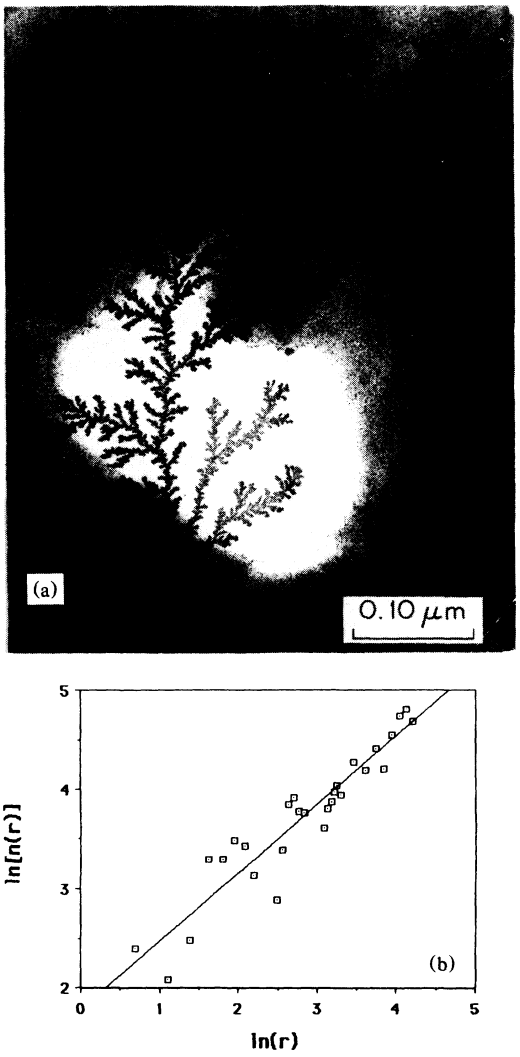

FIG. 4. The fractal dimension of this branch is $D = 1.69 \pm 0.05$.

they crystallized. Why then does an apparently two-dimensional pattern form during crystallization?

Bulk diffusion coefficients of Ge and Se in chalcogenide glasses are extremely small. From the annealing data of Connell[18] we estimate the diffusion coefficient for Se in bulk $GeSe_2$ at 220 °C to be $D_{Se}(220\,^{\circ}C) \cong 3.7 \times 10^{-15}$ cm^2/s.[19] From the observed immobility of Ge diffusing into chalcogenide films, Eickhorn and Frischet set an upper limit on the diffusivity of Ge in $Se_{40}Ge_{40}As_{20}$ at $D_{Ge}(280\,^{\circ}C) \cong 4.9 \times 10^{-16}$ cm^2/s. Because amorphous $GeSe_2$ films have lower defect concentrations than $Se_{40}Ge_{40}As_{20}$, we would expect $D_{Ge}(220\,^{\circ}C)$ to be even smaller in our system.

From the sizes of the observed fractal regions formed during 30-min annealing, we estimate the minimum velocity for the advancing tips to be approximately $v \sim 10$ Å/s. This would suggest a diffusion length shorter than $l = D_{Se}/v \sim 4$ Å. Thus, scale invariant patterns could not have formed through bulk diffusion of atoms.[20]

Surface diffusion coefficients, however, are commonly measured to be 10^8–10^{10} larger than those of the bulk. Advancement of the crystallization front through surface diffusion would account both for the scale invariance of the observed structures and also for their apparent two dimensionality. We conclude that our observations are consistent with diffusion-limited growth in the quasistatic limit.

In a solid-solid phase transition a number of additional factors are expected to affect the results. The specific volume of the crystalline phase is smaller than that of the amorphous state and because of this, long-range elastic forces are created during the growth. It cannot be excluded that these forces themselves may represent an instability and play an important role in the fractal growth. The inhomogeneities of the impurities usually have an effect on the shape of the actual interface as well. However, the latter effect is only local and it is not expected to lead to an inhomogeneous structure on large length scales (unless we have a percolation-like regime close to threshold).

In this paper we have presented an example of the production of a fractal pattern in surface crystallization. This fills a gap in our understanding of the relevance of the DLA model in interfacial pattern formation. This, we believe, is the first well-characterized case of fractal crystallization. We are able to see a fractal here rather than an ordered crystal because the random orientation of the crystallites averages the intrinsic anisotropy. Former experiments in other types of systems[6-13] together with this observation seem to indicate that fractal patterns are ubiquitous in diffusion-limited processes with long diffusion lengths and small anisotropy.

Two of us (L.M.S. and D.G.) are supported by National Science Foundation Grant No. 85-05474. T.V. and L.M.S. would like to thank the Aspen Center for Physics for hospitality.

[1]E. Ben-Jacob, N. D. Goldenfeld, J. S. Langer, and G. Schon, Phys. Rev. Lett. **51**, 1930 (1983).

[2]R. Brower, D. Kessler, J. Koplik, and H. Levine, Phys. Rev. Lett. **51**, 1111 (1983).

[3]L. M. Sander, P. Ramanlal, and E. Ben-Jacob, Phys. Rev. A **32**, 3160 (1985).

[4]T. A. Witten and L. M. Sander, Phys. Rev. Lett. **47**, 1400 (1981); Phys. Rev. B **28**, 5686 (1986).

[5]B. Mandelbrot, *The Fractal Geometry of Nature* (Freeman, San Francisco, 1982).

[6]J. Nittmann, G. Daccord, and H. E. Stanley, Nature (London) **314**, 141 (1985).

[7]E. Ben-Jacob, R. Godbey, N. Goldenfeld, J. Koplik, H. Levine, and L. Sander, Phys. Rev. Lett. **55**, 1315 (1985).

[8]J. D. Chen and D. Wilkinson, Phys. Rev. Lett. **55**, 2688 (1985).

[9]K. J. Maloy, J. Feder, and T. Jossang, Phys. Rev. Lett. **55**, 2688 (1985).

[10]M. Matsushita, M. Sano, Y. Hayakawa, H. Honjo, and

Y. Sawada, Phys. Rev. Lett. **53**, 286 (1984).
[11]D. Grier, L. M. Sander, Roy Clarke, and E. Ben-Jacob, Phys. Rev. Lett. **56**, 1264 (1986).
[12]Y. Sawada, A. Dougherty, and J. P. Gollub, Phys. Rev. Lett. **56**, 1260 (1986).
[13]R. Brady and R. C. Ball, Nature (London) **309**, 225 (1984).
[14]W. T. Elam, S. A. Wolf, J. Sprague, D. V. Gubser, D. Van Vechten, G. L. Barz, and P. Meakin, Phys. Rev. Lett. **54**, 701 (1985).
[15]R. Azovlay, H. Thibierge, and A. Brenac, J. Non-Cryst. Solids **18**, 33 (1975).
[16]J. S. Langer, Rev. Mod. Phys. **52**, 1 (1980).
[17]M. E. Glicksman, Mater. Sci. Eng. **65**, 45 (1984).
[18]G. A. N. Connell, Phys. Rev. B **24**, 4560 (1981).
[19]U. Eichhorn and G. H. Frischet, J. Non-Cryst. Solids **30**, 211 (1978), give diffusivities of Ge and Se in amorphous $Se_{40}Ge_{40}As_{20}$ at 280 °C as $D_{Ge}=4.9\times10^{-16}\cdot cm^2/s$, $D_{Se}=4.3\times10^{-15}\,cm^2/s$.
[20]M. Nauenberg, R. Richter, and L. Sander, Phys. Rev. B **28**, 1649 (1983).

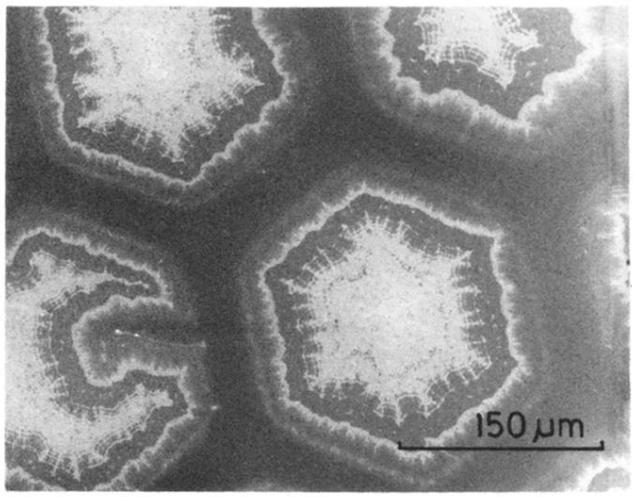

FIG. 1. Picture of the heat-treated (220 °C, 1 h) $GeSe_2$ film previously deposited on carbon layer supported by a honeycomb copper mesh. This image was obtained by a transmission electron microscope. The crystallization starts in concentric rings.

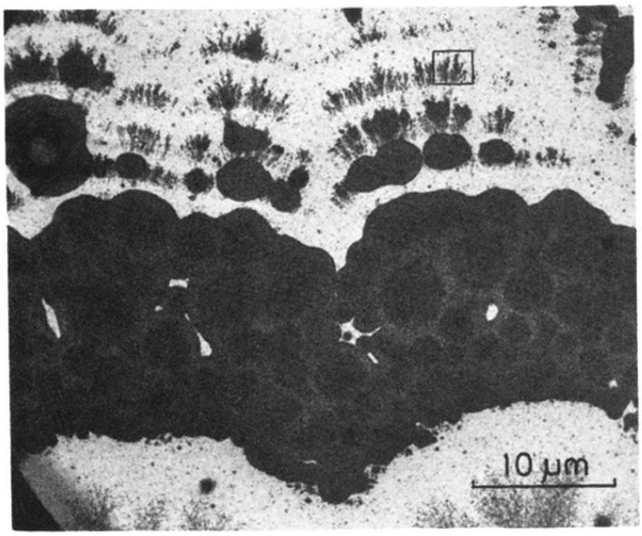

FIG. 2. Fragment of Fig. 1. Two types of crystallization fronts appear in the amorphous regions: (i) dendritic growth, (ii) spherolitic crystallization (the darkest part of the picture). Figs. 3 and 4 are enlargements from the interior of the small box.

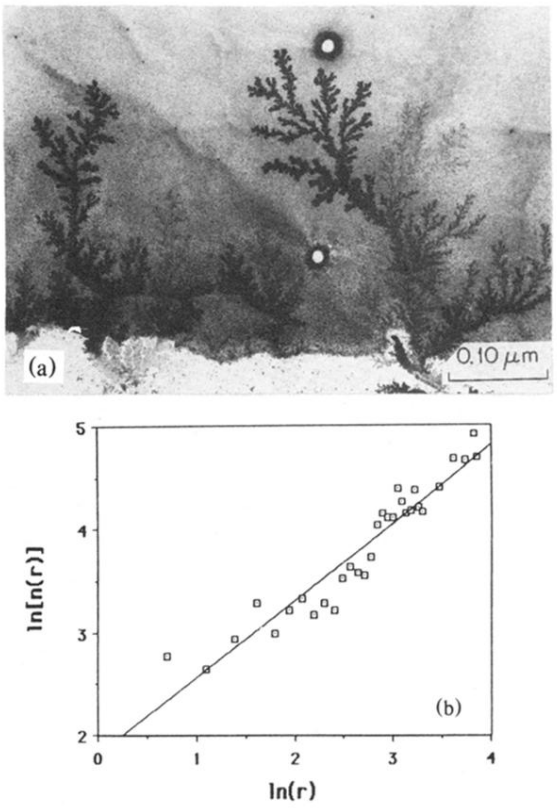

FIG. 3. (a) Part of the forest of dendritic crystals grown in the first zone. These trees are polycrystalline with a characteristic crystallite size less than 1000 Å. This size is considerably smaller than the width of the branches. (b) The two new branches have fractal dimension $D = 1.73 \pm 0.05$.

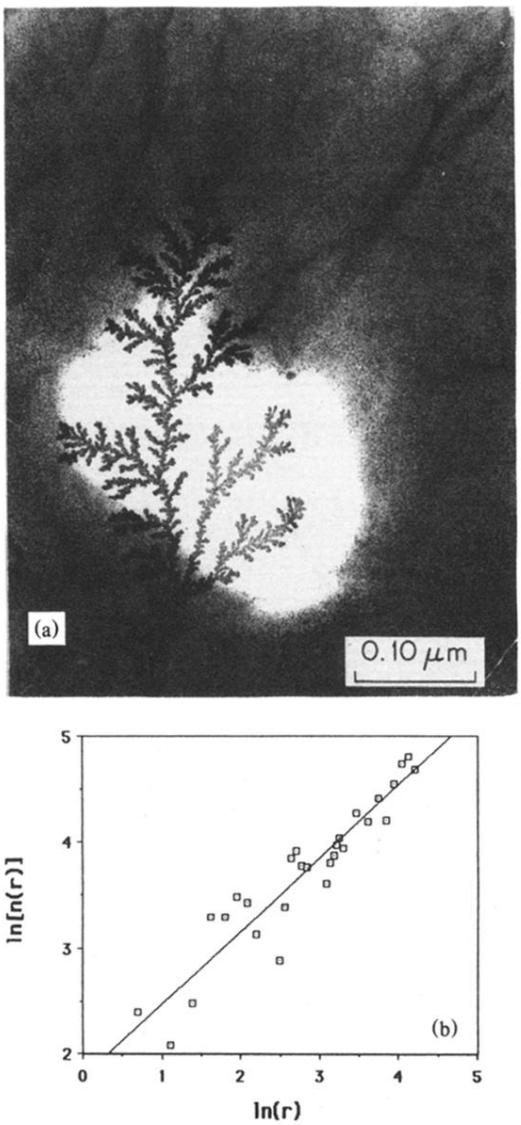

FIG. 4. The fractal dimension of this branch is $D = 1.69 \pm 0.05$.